Article

Cell Reports

Absence of Neurofibromin Induces an Oncogenic Metabolic Switch via Mitochondrial ERK-Mediated Phosphorylation of the Chaperone TRAP1

Graphical Abstract

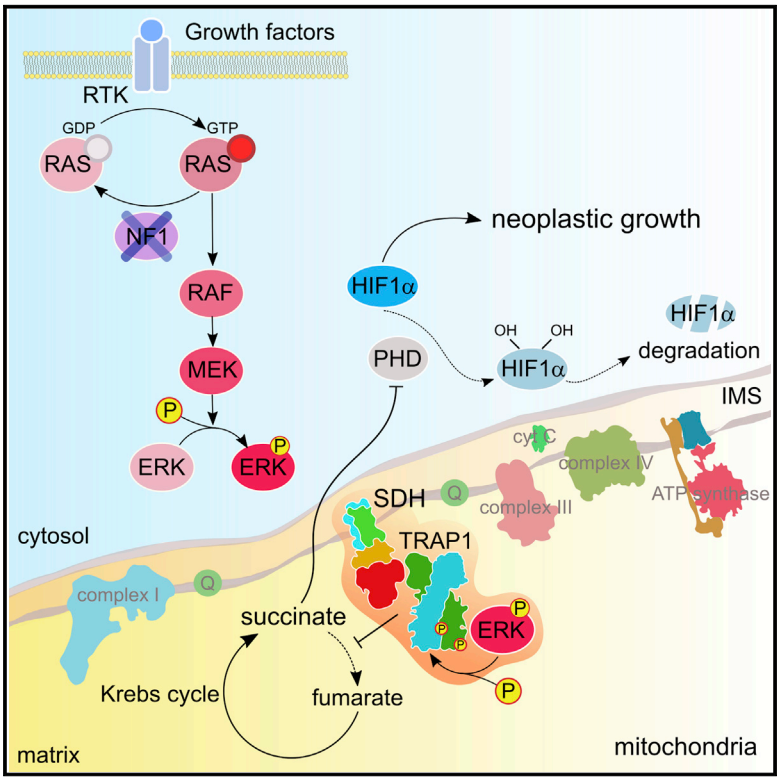

Highlights

- Cells lacking neurofibromin exhibit decreased respiration
- ERK1/2 inhibits respiratory complex II (SDH) via phosphorylation of the chaperone TRAP1
- SDH inhibition by ERK1/2 phosphorylation of TRAP1 is mandatory for neoplastic growth

Authors

Ionica Masgras, Francesco Ciscato, Anna Maria Brunati, ..., Fiorella Calabrese, Paolo Bernardi, Andrea Rasola

Correspondence

andrea.rasola@unipd.it

In Brief

Induction of the Ras/ERK signaling pathway characterizes many tumors and leads to metabolic changes whose oncogenic relevance is unclear. Masgras et al. reveal that ERK1/2 orchestrates a metabolic switch through phosphorylation of the mitochondrial chaperone TRAP1 and the ensuing inhibition of respiratory complex II that crucially contributes to neoplastic growth.

Masgras et al., 2017, Cell Reports *18*, 659–672
January 17, 2017
http://dx.doi.org/10.1016/j.celrep.2016.12.056

CellPress

Cell Reports
Article

OPEN ACCESS
CellPress

Absence of Neurofibromin Induces an Oncogenic Metabolic Switch via Mitochondrial ERK-Mediated Phosphorylation of the Chaperone TRAP1

Ionica Masgras,[1] Francesco Ciscato,[1] Anna Maria Brunati,[2] Elena Tibaldi,[2] Stefano Indraccolo,[3] Matteo Curtarello,[3] Federica Chiara,[4] Giuseppe Cannino,[1] Elena Papaleo,[5] Matteo Lambrughi,[5] Giulia Guzzo,[1] Alberto Gambalunga,[4] Marco Pizzi,[6] Vincenza Guzzardo,[6] Massimo Rugge,[6] Stefania Edith Vuljan,[4] Fiorella Calabrese,[4] Paolo Bernardi,[1] and Andrea Rasola[1,7,*]

[1]CNR Institute of Neuroscience and Department of Biomedical Sciences, University of Padova, 35131 Padova, Italy
[2]Department of Molecular Medicine, University of Padova, 35131 Padova, Italy
[3]Istituto Oncologico Veneto, IRCCS, 35128 Padova, Italy
[4]Department of Cardiac, Thoracic, and Vascular Sciences, University of Padova, 35128 Padova, Italy
[5]Computational Biology Laboratory, Unit of Statistics, Bioinformatics and Registry, Danish Cancer Society Research Center, 2100 Copenhagen, Denmark
[6]Department of Medicine, University of Padova, 35128 Padova, Italy
[7]Lead Contact
*Correspondence: andrea.rasola@unipd.it
http://dx.doi.org/10.1016/j.celrep.2016.12.056

SUMMARY

Mutations in neurofibromin, a Ras GTPase-activating protein, lead to the tumor predisposition syndrome neurofibromatosis type 1. Here, we report that cells lacking neurofibromin exhibit enhanced glycolysis and decreased respiration in a Ras/ERK-dependent way. In the mitochondrial matrix of neurofibromin-deficient cells, a fraction of active ERK1/2 associates with succinate dehydrogenase (SDH) and TRAP1, a chaperone that promotes the accumulation of the oncometabolite succinate by inhibiting SDH. ERK1/2 enhances both formation of this multimeric complex and SDH inhibition. ERK1/2 kinase activity is favored by the interaction with TRAP1, and TRAP1 is, in turn, phosphorylated in an ERK1/2-dependent way. TRAP1 silencing or mutagenesis at the serine residues targeted by ERK1/2 abrogates tumorigenicity, a phenotype that is reverted by addition of a cell-permeable succinate analog. Our findings reveal that Ras/ERK signaling controls the metabolic changes orchestrated by TRAP1 that have a key role in tumor growth and are a promising target for anti-neoplastic strategies.

INTRODUCTION

Deregulated induction of Ras/ERK signaling stimulates several biological processes that are crucial for neoplastic growth, including cellular proliferation, suppression of cell death, and acquisition of invasive, metastatic, and pro-angiogenic properties by tumor cells (Dhillon et al., 2007). One mechanism to enhance signaling through the Ras /ERK transduction pathway is constituted by inactivation of neurofibromin, a Ras-GTPase-activating protein (Ras-GAP) (Yap et al., 2014) that inhibits the proto-oncogene Ras by increasing the intrinsic GTPase activity of its active, GTP-bound form (Ahearn et al., 2011). Neurofibromin is the product of the tumor suppressor gene NF1, whose loss-of-function mutations cause neurofibromatosis type 1 (NF1), an autosomal-dominant, tumor-predisposing genetic syndrome that affects about 1 in 3,000 individuals worldwide (Lin and Gutmann, 2013). Biallelic inactivating mutations at the NF1 locus induce the formation of a variety of tumor types; among these are neurofibromas, benign tumors that develop within perineural sheaths of peripheral nerves and are the hallmark of NF1. A subset of neurofibromas (called plexiform) grow in peripheral nerve bundles and can undergo transformation into highly aggressive sarcomas (Brems et al., 2009). In addition, NF1 patients have an increased risk of developing a variety of other tumor types, such as glioma, leukemia, pheochromocytoma, gastrointestinal stromal tumor, rhabdomyosarcoma, and breast cancer (Lin and Gutmann, 2013). Moreover, NF1 is one of the most frequently mutated genes in several sporadic malignancies, including lung, breast, ovarian, pancreatic, and prostate cancer, where NF1 mutations are frequently associated with resistance to therapy and a poor outcome (reviewed in Ratner and Miller, 2015).

Even if Ras controls the downstream activation of multiple effectors (Karnoub and Weinberg, 2008), and neurofibromin is involved in a number of Ras-independent signaling pathways (Ratner and Miller, 2015), it is believed that tumorigenesis caused by lack of neurofibromin specifically requires the deregulated activation of signaling through the Ras/ERK transduction axis because its inhibition leads to a remarkable anti-neoplastic effect in several NF1-related tumor models (Barkan et al., 2006; Jessen et al., 2013; Malone et al., 2014; See et al., 2012).

The Ras/ERK signaling pathway contributes to the metabolic reprogramming that allows neoplastic cells to thrive under the

conditions of limited oxygen supply that they encounter during neoplasm accrual (Pylayeva-Gupta et al., 2011; White, 2013). These metabolic changes are characterized by a partial inhibition of mitochondrial oxidative phosphorylation (OXPHOS) (Barbosa et al., 2012) as well as by enhanced utilization of glucose and glutamine for anabolic needs, induction of anti-oxidant defenses, and anaplerotic supply of the mitochondrial tricarboxylic acid (TCA) cycle that is required to maintain both energy homeostasis and several biosynthetic pathways (Boroughs and DeBerardinis, 2015). The mechanisms by which oncogenic activation of the Ras/ERK pathway promotes this rearrangement of metabolic circuitries are only partially understood (White, 2013), and it remains to be established whether any Ras/ERK-dependent metabolic derangement occurs in tumors related to neurofibromin loss of function and is required for their progression.

The Ras/ERK pathway has a mitochondrial branch (Zhu et al., 2003; Poderoso et al., 2008) whose anti-apoptotic functions can contribute to cell tumorigenicity (Rasola et al., 2010). Many crucial bioenergetic processes are located in mitochondria or have mitochondrial components, and mitochondria can play a promoter role in the tumorigenic process through accumulation of oncometabolites; i.e., metabolites that contribute to tumorigenesis via regulation of transcription factors or epigenetic changes (Yang et al., 2013). One such oncometabolite is succinate; an increase in its intracellular levels causes pseudohypoxia by stabilizing the hypoxia-inducible transcription factor (HIF-1) independently of oxygen tension (Selak et al., 2005). The subsequent activation of the HIF-1-responsive genes leads to further metabolic changes and to induction of both angiogenesis and epithelial-mesenchymal transition (LaGory and Giaccia, 2016; Semenza, 2013), thus orchestrating progression to malignancy. It was proposed that Ras/ERK signaling might promote metabolic changes through HIF-1 activation (Blum et al., 2005; White, 2013). However, whether the mitochondrial Ras/ERK axis directly takes part in the mitochondrial metabolic rewiring associated with neoplastic transformation is not known.

Succinate accumulation can be caused by inactivating mutations in genes encoding succinate dehydrogenase (SDH), an enzyme that catalyzes both the oxidation of succinate to fumarate and the transfer of electrons to the quinone pool of the respiratory chain (Cecchini, 2003), therefore being placed at the crossroad between the TCA cycle and OXPHOS. Such mutations are found in a panel of tumors that partially overlap with those associated with NF1; they include paragangliomas, phaeochromocytomas, gastrointestinal stromal tumors, renal and thyroid tumors, and neuroblastomas (Bardella et al., 2011; Hoekstra and Bayley, 2013). We have previously demonstrated that a pro-neoplastic increase in intracellular succinate levels can also be prompted by the inhibitory interaction between SDH and the mitochondrial chaperone TRAP1, which leads to HIF-1α stabilization and is required for tumor growth (Sciacovelli et al., 2013). The TRAP1 level has been found to be increased in several types of tumors (Kang et al., 2007). Furthermore, it was observed that it is phosphorylated by Ser/Thr kinases (Condelli et al., 2015; Pridgeon et al., 2007), but it is unknown whether TRAP1 can be the target of kinase pathways that are aberrantly activated in tumor cells. Thus it remains unexplored whether and how TRAP1 phosphorylation might contribute to the process of neoplastic growth.

Here we provide a mechanistic connection between deregulated activation of Ras/ERK signaling and the pro-neoplastic metabolic switch orchestrated by TRAP1. Our observations demonstrate that active ERK1/2 interacts with TRAP1 and SDH in mitochondria of neurofibromin-deficient cells and that ERK-dependent phosphorylation of specific residues on TRAP1 has a key role in their tumorigenicity.

RESULTS

Lack of Neurofibromin Changes the Bioenergetic Properties of Cells

We studied the metabolic profile of mouse embryonic fibroblasts (MEFs) derived from both wild-type mice and syngenic Nf1-knockout animals ($Nf1^{+/+}$ and $Nf1^{-/-}$ MEFs, respectively) (Shapira et al., 2007; Figure S1A). $Nf1^{-/-}$ MEFs had a higher glycolytic activity than their wild-type counterparts, as demonstrated both by the rise in the extracellular acidification rate following glucose administration (Figure 1A) and by measurements of glucose-dependent ATP synthesis (Figure 1B). Moreover, oxygen consumption rate (OCR) experiments revealed that both basal and coupled respiration as well as maximal and spare respiratory capacity were lower in $Nf1^{-/-}$ than in $Nf1^{+/+}$ MEFs (Figures 1C and 1D; Figure S1B). No differences in mitochondrial morphology, mass, or membrane potential were detected between MEFs with or without neurofibromin (Figures S1C and S2A–S2C). Taken together, these data indicate that lack of neurofibromin per se is sufficient to induce a metabolic shift of cells toward the Warburg-like phenotype that characterizes many tumor cell types, which is endowed with enhanced glucose usage and diminished OXPHOS.

ERK1/2 Activity Prompted by Lack of Neurofibromin Regulates Mitochondrial Bioenergetics

We analyzed the influence of neurofibromin loss on ERK1/2 activity in MEFs. As expected, $Nf1^{-/-}$ MEFs displayed a constitutively higher level of ERK1/2 phosphorylation than their wild-type counterparts and underwent a much stronger ERK1/2 induction after growth factor stimulation (Figure 2A). We had previously observed that, in several cell types, a fraction of ERK1/2 is located in mitochondria and that the activity of this mitochondrial ERK1/2 can contribute to the survival of tumor cells exposed to stress conditions (Masgras et al., 2012; Rasola et al., 2010). Here we found a fraction of active ERK1/2 in mitochondria of cell types that lack neurofibromin, including $Nf1^{-/-}$ MEFs (Figure 2B), cells from human plexiform neurofibromas (Figure 2C), and U87 cells (Figure S1A; Figure 2D) that derive from a human glioblastoma; i.e., a tumor type frequently associated with loss of neurofibromin (Cancer Genome Atlas Research Network, 2008; Hollstein and Cichowski, 2013). We inhibited ERK1/2 activity in $Nf1^{-/-}$ MEFs either through administration of PD98059, an inhibitor of the upstream kinase MEK (Figure S2D), or through expression of a dominant-negative MEK1 protein (MEK1-DN) (Figure S2E). Conversely, we activated ERK1/2 in $Nf1^{+/+}$ MEFs by expressing a constitutively active MEK1 protein (MEK1-CA) (Figure S2E). We found that MEK1 inhibition, which

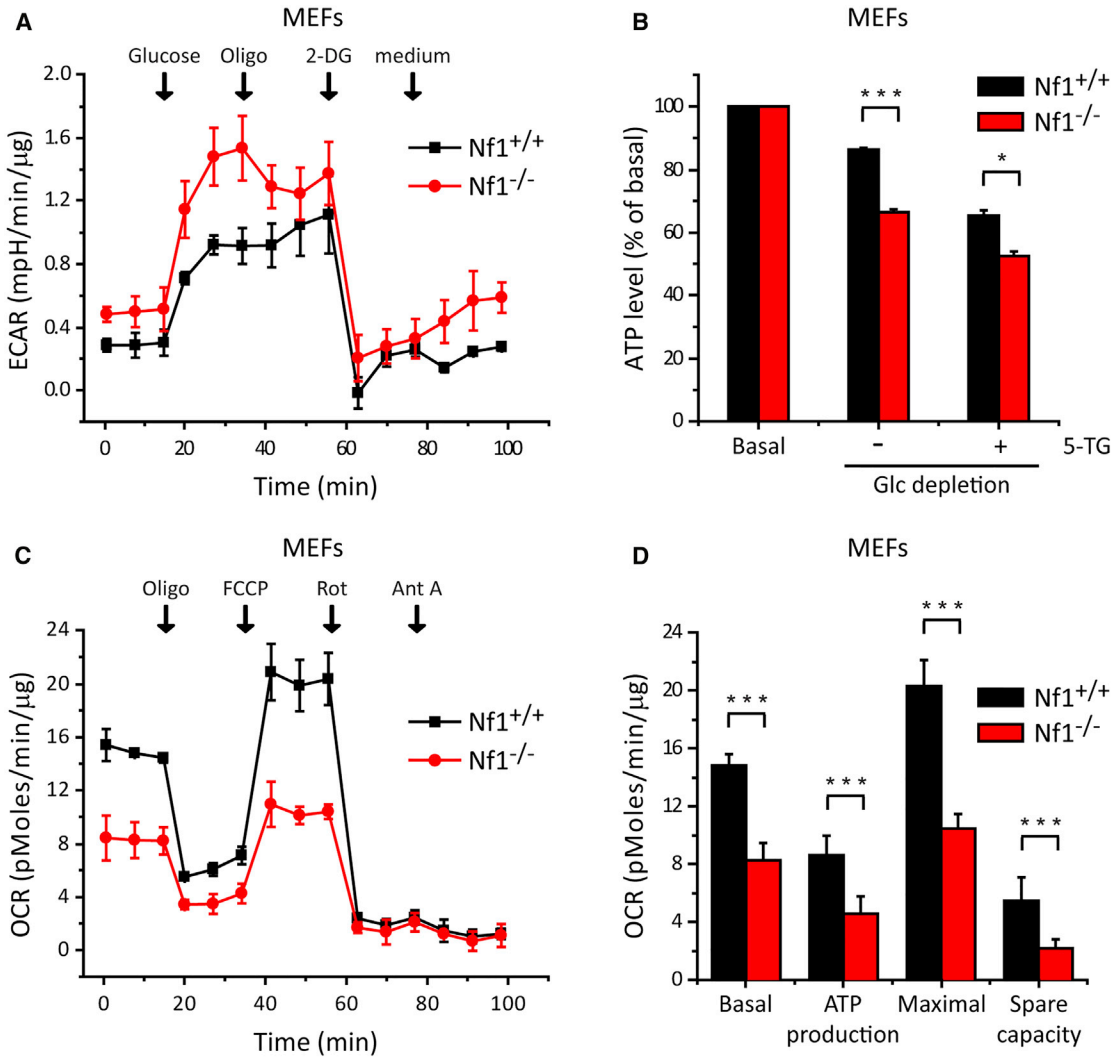

Figure 1. The Absence of Neurofibromin Changes the Bioenergetics of MEFs

(A) Representative measurements of the extracellular acidification rate (ECAR) performed on MEF monolayers. Subsequent additions of glucose, the ATP synthase inhibitor oligomycin, and the hexokinase inhibitor 2-deoxy-glucose (2-DG) were carried out where indicated.

(B) ATP levels were measured in $Nf1^{+/+}$ and $Nf1^{-/-}$ MEFs kept under standard culture conditions (bars on the left) or undergoing 2-hr glucose depletion with or without the hexokinase inhibitor 5-thio-glucose (5-TG).

(C and D) Representative traces (C) and quantification (D) of the oxygen consumption rate (OCR) in MEFs. Subsequent additions of oligomycin, which allows determination of respiration coupled to ATP synthesis, of the proton uncoupler carbonyl cyanide-4-(trifluoromethoxy)phenylhydrazone (FCCP), which indicates the maximal and the spare respiratory capacity, and of the respiratory complex I and III inhibitors rotenone and antimycin A, respectively, were carried out as indicated.

Data are reported as mean ± SD values ($n \geq 3$); asterisks indicate significant differences (**$p < 0.01$, *$p < 0.05$; Student's t test analysis). See also Figures S1 and S2.

did not alter, per se, either the mass or membrane potential of mitochondria (Figures S2A–S2C), increased the OCR both in $Nf1^{-/-}$ MEFs (Figures 2E and 2F; Figure S2F) and in U87 glioblastoma cells (Figures 2G and 2H). In the mirror experiment, ERK1/2 activation by MEK1-CA expression markedly decreased the OCR of $Nf1^{+/+}$ MEFs, making them reach a respiratory profile similar to that of MEFs lacking neurofibromin (Figures 2E and 2F; Figure S2F).

These results indicate that deregulated activation of the Ras/ERK signaling pathway in neurofibromin-deficient cells is responsible for a metabolic rearrangement characterized by a decrease in mitochondrial OXPHOS.

Mitochondrial ERK1/2 Inhibits SDH following Interaction with TRAP1

We then asked whether ERK1/2 could alter the mitochondrial bioenergetics of neurofibromin-deficient cells by directly interacting with any OXPHOS complex. We found that ERK1/2 associated both with the respiratory complex II, also known as SDH, and with the mitochondrial chaperone TRAP1 in $Nf1^{-/-}$ MEFs

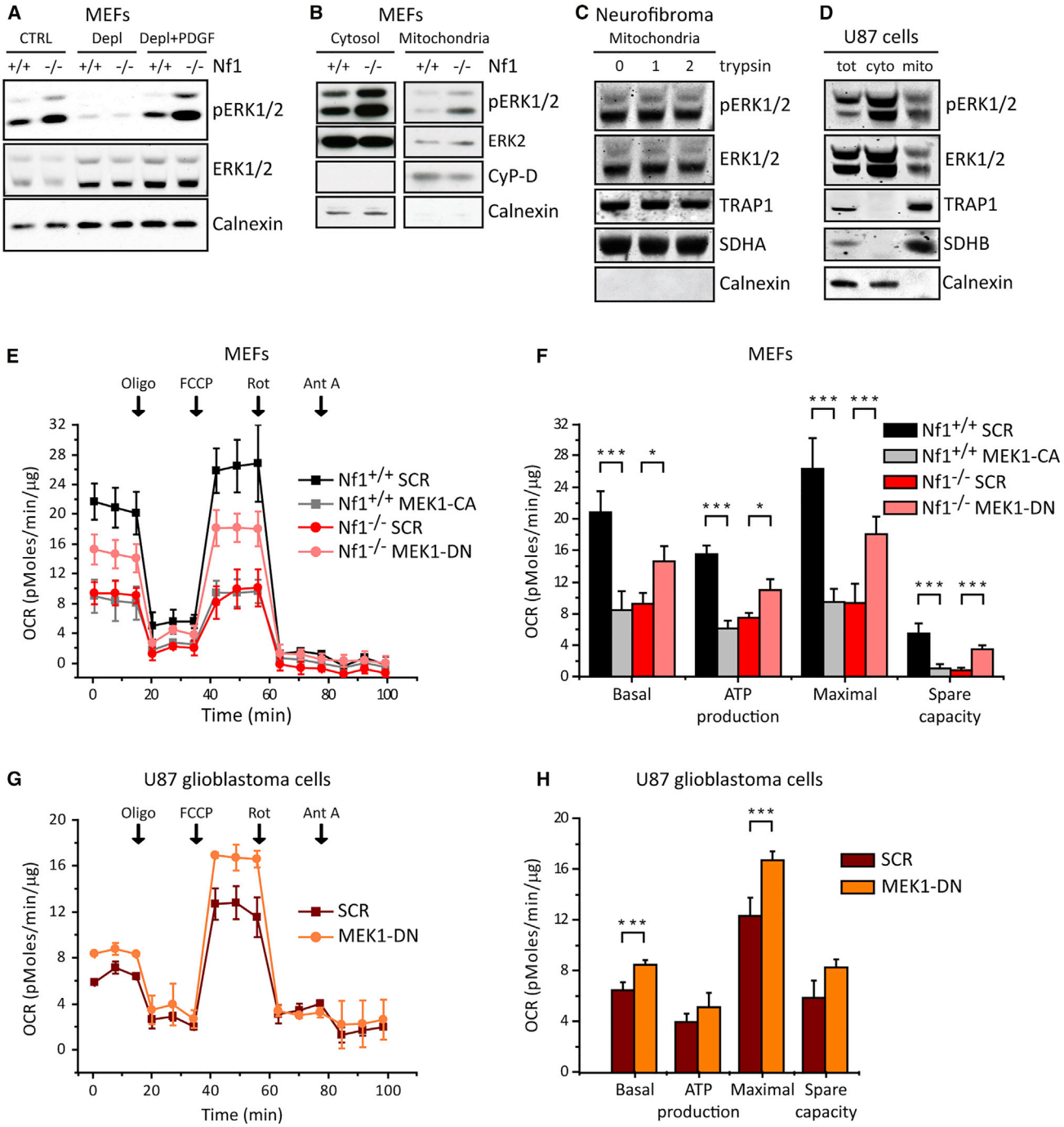

Figure 2. Active ERK1/2 Is in Mitochondria of Cells Lacking Neurofibromin and Regulates Their Bioenergetic Features

(A) Changes in ERK1/2 phosphorylation following 2-hr serum depletion of $Nf1^{+/+}$ and $Nf1^{-/-}$ MEFs and subsequent exposure to PDGF (10 ng/ml, 10 min); calnexin was used as a loading control.

(B–D) Expression of active, phosphorylated ERK1/2 was assessed in the cytosolic and mitochondrial fractions of MEFs (B), in mitochondria from a representative plexiform neurofibroma (C), and in the cytosolic and mitochondrial fractions of U87 human glioblastoma cells (D). Cyclophilin D (CyP-D), TRAP1, and SDH subunits A (SDHA) and B (SDHB) were used as mitochondrial markers; calnexin was used as an indicator of the presence of non-mitochondrial proteins.

(E–H) Representative traces (E and G) and quantification (F and H) of the OCR are shown as in Figure 1. In (E) and (F), experiments were conducted on $Nf1^{+/+}$ and $Nf1^{-/-}$ MEFs and in (G) and (H) on U87 glioblastoma cells; where indicated, cells expressed the constitutively active or the dominant-negative MEK1 protein (MEK1-CA and MEK1-DN, respectively).

Data are reported as mean ± SD values ($n \geq 3$); asterisks indicate significant differences (***$p < 0.01$, *$p < 0.05$; Student's t test analysis). See also Figures S1 and S2.

(Figures 3A–3C; Figures S3A–S3B); no interaction could be detected between ERK1/2 and any other OXPHOS component (data not shown). In cells lacking neurofibromin, the phosphorylated, active form of ERK1/2 was part of this multimeric complex, whereas it was barely detectable in $Nf1^{+/+}$ MEFs, in which the interaction among these proteins was weaker (Figure 3C; Figure S3A). Moreover, in vitro phosphorylation shifted TRAP1, SDH, and ERK1/2 to high-molecular-weight complexes in mitochondria of $Nf1^{-/-}$ MEFs, whereas phosphatase treatment enhanced the dissociation of such multimers (Figure 3A). These data, together with the observation that inhibition of phosphorylation does not affect the interaction between TRAP1 and either SDH or ERK1/2 (Figure 3B; Figure S3B), suggest that a phosphorylation-dependent process is specifically involved in the formation of large complexes among these proteins.

The succinate:coenzyme Q reductase (SQR) enzymatic activity of SDH was lower in $Nf1^{-/-}$ than in $Nf1^{+/+}$ MEFs (Figure 3D). We also found that SQR activity inversely correlated with ERK1/2 induction in $Nf1^{-/-}$ MEFs; it increased under starvation conditions, where ERK1/2 was completely inhibited, whereas the subsequent PDGF treatment, which strongly activated ERK1/2, lowered SQR activity back to its basal level (compare Figure 3E with Figure 2A for ERK1/2 modulation). These data indicated that ERK1/2 activation could downregulate SDH activity and were corroborated by the observation that expression of a kinase-dead ERK2 enzyme increased the SQR activity of SDH in neurofibromin-deficient cells (Figure 3F), whereas $Nf1^{+/+}$ MEFs expressing a MEK1-CA protein showed SQR inhibition (Figure 3G). Modulation of SDH activity by the Ras/ERK pathway was independent of changes in SDH protein levels; these were not affected either by the absence of neurofibromin or by inhibition of the Ras/ERK pathway (Figure S2B). Moreover, TRAP1 expression levels were similar in $Nf1^{+/+}$ and $Nf1^{-/-}$ MEFs (Figure S3B). Like in $Nf1^{-/-}$ MEFs, we found that active ERK1/2, TRAP1, and SDH also interacted in human U87 glioblastoma cells (Figure 3H), and expression of a kinase-dead ERK2 protein that partially localized in mitochondria did not change the protein levels of SDH (Figure S3D) but increased its SQR enzymatic activity (Figure 3I).

TRAP1 Is Phosphorylated in an ERK-Dependent Way

To further elucidate the functional meaning of the interaction between mitochondrial ERK1/2 and TRAP1, we investigated whether TRAP1 was an ERK1/2 phosphorylation target. We found that TRAP1 was Ser/Thr-phosphorylated after treatment with platelet-derived growth factor (PDGF) or expression of wild-type ERK and that TRAP1 phosphorylation was decreased both under starvation and upon expression of the kinase-dead ERK2 protein (Figures 4A and 4B). It was shown that the chaperone activity of TRAP1 is enhanced after heat shock up to 55°C (Leskovar et al., 2008 and unpublished data). We reasoned that, under these conditions, TRAP1 interactors and TRAP1-dependent regulatory events would be selectively preserved, whereas the conformation and activity of non-chaperoned mitochondrial proteins would be lost. Accordingly, after a short heat shock, both TRAP1 and ERK1/2 were maintained in the soluble fraction, whereas mitochondrial Akt was not detectable anymore (Figure S4A). Notably, after the heat shock we could detect both active ERK1/2 (Figures S4A and S4B) and phosphorylated TRAP1 (Figures 4C and 4D; Figures S4A and S4B). TRAP1 phosphorylation was markedly decreased both by the wide-spectrum kinase inhibitor staurosporine and in the presence of a kinase-dead form of ERK2 (Figures 4C and 4D; Figure S4B).

These data strongly support the hypothesis that TRAP1 is phosphorylated in an ERK1/2-dependent way. Hence, to determine ERK1/2 target residues on TRAP1, we crossed data obtained with the platforms Prediction of PK-Specific Phosphorylation Site (http://ppsp.biocuckoo.org/) and Phospho Site Plus (http://www.phosphosite.org/), finding Ser226, Ser511, and Ser568 to be potential ERK phosphorylation sites on human TRAP1. We then measured the solvent accessibility of these sites using all-atom explicit solvent molecular dynamics (MD) simulation either for the apo and ADP-bound form of the chaperone to account for the fluctuations around the native state of the protein. We selected the only full-length and dimeric 3D structure available so far in the PDB for TRAP1, that of *Danio rerio* (Lavery et al., 2014), in which Ser511 and Ser568 are replaced by Ser526 and Ser582, respectively, whereas Ser226 is substituted by Ala241. The most accessible phospho site and, thus, available for a kinase independently of the cofactor-bound state of the protein in the simulations of the closed state of the protein was Ser582 (Ser568 in Figure 4E and Table S1). Furthermore, Ser582 was the only site whose phosphorylation was not expected to destabilize the protein because the $\Delta\Delta G$ between the folded and unfolded state upon phosphorylation was 0.77 kcal/mol, whereas phosphorylation at the other two sites induced a destabilizing $\Delta\Delta G$ of more than 3.8 kcal/mol in the closed state of the chaperone, in agreement with the fact that these sites are partially buried in the closed structure. However, TRAP1 has been suggested to undergo large conformational changes during the catalytic cycle, converting from closed states (as the ones simulated here) to open states, as also observed in other chaperones (Krukenberg et al., 2011; Lavery et al., 2014). The destabilization of the closed state predicted by the $\Delta\Delta G$ calculations suggested that phosphorylation at Ser526 was favored in the open state. We thus built a model of the open conformation of TRAP1 in its apo state based on the structure of *E.coli* HSP90 (PDB: 2IOQ; Shiau et al., 2006), and the location of Ser511 (Ser526 in Figure 4F) suggested that its accessibility could be modulated by opening/closing motions of the chaperone, increasing more than 10-fold in the model of the open state.

These predictions were confirmed by a marked decrease in the phosphorylation of TRAP1 following Ser-to-Ala mutagenesis both at the 511 and at the 568 residue (Figure 4G). Interestingly, both mutants markedly decreased the capability to form high molecular complexes with ERK1/2 and SDH (compare Figure 4H and Figure S4C with Figure 3A). We also observed that inhibition of the TRAP1 chaperone cycle with the use of 17-(Allylamino)geldanamycin (17-AAG) dissociates it from ERK1/2, whereas the complex was maintained in the presence of the kinase inhibitor staurosporine (Figures 4I and 3B). The ERK capability to phosphorylate TRAP1 was not affected by 17-AAG when the latter was added after heating (Figures 4I; Figure S4B), but treatment with 17-AAG before the heat shock induced the dissociation of TRAP1 from ERK1/2, thus allowing ERK1/2 degradation (Figure 4I).

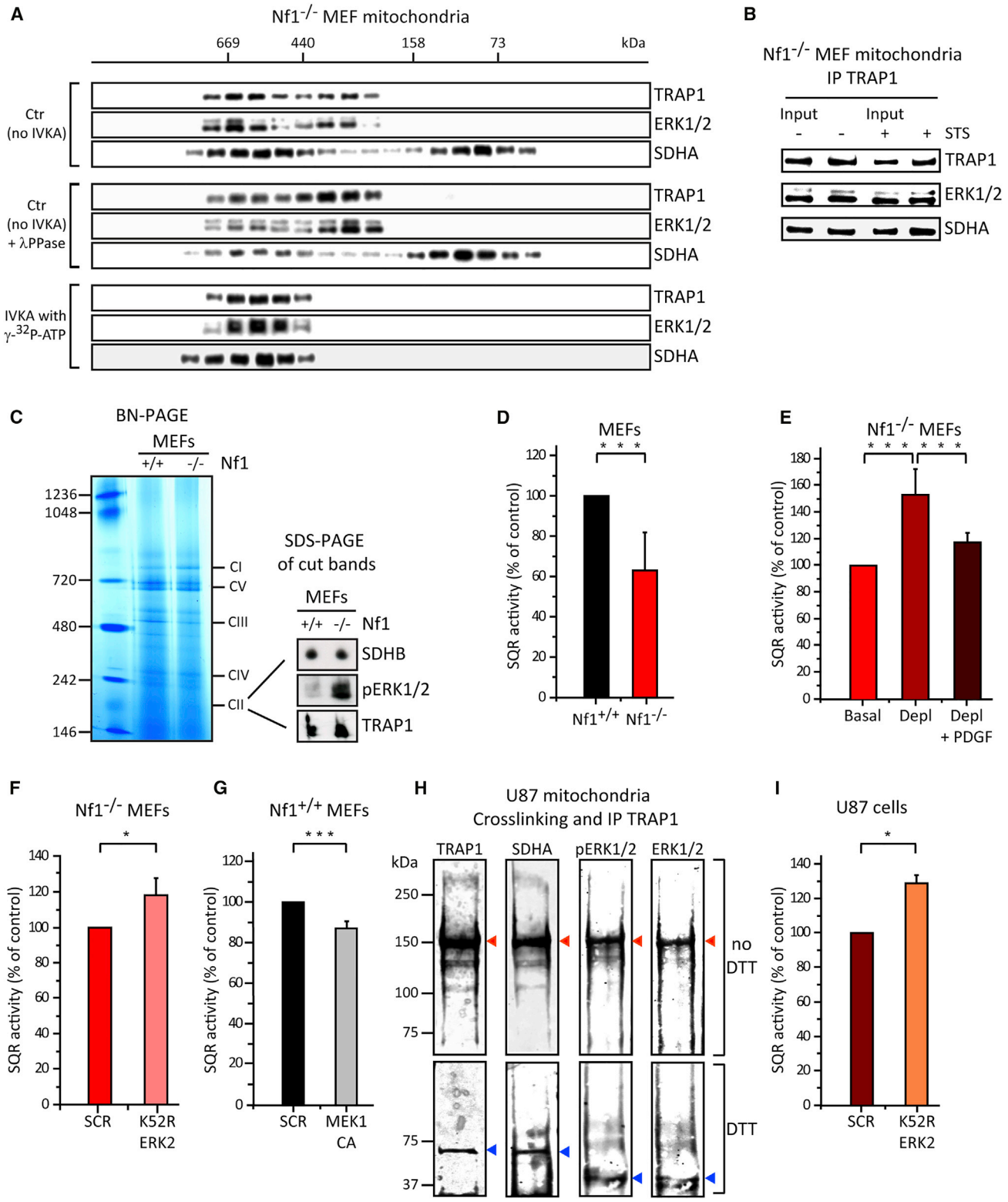

Figure 3. ERK1/2 Interacts with TRAP1 and SDH in Mitochondria of Cells Lacking Neurofibromin and Downmodulates Their SQR Enzymatic Activity

(A) Gel filtration chromatography analysis of TRAP1, ERK1/2, and SDHA distribution in Nf1$^{-/-}$ MEF mitochondria. Mitochondrial extracts were left untreated (top), exposed to lambda phosphatase (λPPase, center), or underwent an in vitro kinase assay (IVKA, bottom).

(legend continued on next page)

Taken together, these observations indicate that TRAP1 phosphorylation occurs in neurofibromin-deficient cells upon ERK activation and that, in turn, TRAP1 acts as a chaperone to maintain ERK1/2 activity in mitochondria. It was therefore pivotal to understand whether this multimeric complex affected the oncogenic potential of cells lacking neurofibromin.

ERK-Dependent Phosphorylation of TRAP1 Is Required for Its Oncogenic Activity through Inhibition of SDH and Prolyl Hydroxylases

It was shown that activation of Ras/ERK signaling is mandatory for the growth of NF1-related tumors (Barkan et al., 2006; Jessen et al., 2013; Malone et al., 2014; See et al., 2012) even though any characterization of their metabolic features is missing. We found that lack of neurofibromin conferred tumorigenicity to MEFs both in vitro and in vivo (Figures 5A–5C). The oncogenic importance of the Ras/ERK transduction pathway in this model was highlighted by the observation that MEK inhibition blunted the ability of $Nf1^{-/-}$ MEFs to grow in soft agar (Figures 5A and 5B) without affecting cell viability per se (Figure S5A), whereas ERK1/2 induction by expression of MEK1-CA was sufficient to elicit formation of colonies by $Nf1^{+/+}$ MEFs (Figure 5B). Similarly, the tumorigenic properties of U87 glioblastoma cells were inhibited by blocking the Ras/ERK transduction pathway (Figure S5B). Tumors formed by $Nf1^{-/-}$ MEFs following injection in nude mice were exclusively formed by cells lacking neurofibromin (Figure 5C) that were endowed with the presence of TRAP1 and an active ERK1/2 in mitochondria (Figure 5D) and with induction of both HIF-1α and of the lactate transporter MCT4 (Figure 5E), a HIF-1α transcriptional target that is a marker of a metabolic shift toward a Warburg phenotype.

We then assessed the role of TRAP1 in the tumorigenicity of cells lacking neurofibromin. In accord with our previous results in other cell models (Sciacovelli et al., 2013), TRAP1 silencing (Figures S6A–S6C) increased cell respiratory capacity (Figure S6D) and abrogated both the ability of cells to form colonies in soft agar (Figure 6A; Figure S6E) and in vivo tumor growth (Figure 6B).

We had previously shown that TRAP1 prompts a succinate-dependent inhibition of prolyl hydroxylase (PHD) that is pro-neoplastic by hampering the proteasomal degradation of HIF-1α (Sciacovelli et al., 2013). Accordingly, the tumorigenicity of TRAP1-silenced cells lacking neurofibromin was restored by the supply of a cell-permeable succinate analog (dimethyl succinate, DMS) (Figure 6C; Figures S6F and S6G), which inhibits PHD. The capability to form colonies after DMS treatment was abrogated by a cell-permeable form of a-ketoglutarate (1-trifluoromethylbenzyl-a-ketoglutarate, TaKG), which reverses HIF-1α stabilization by restoring PHD enzymatic activity (Figure 6C; Figure S6G).

We also found that ERK-dependent phosphorylation of TRAP1 was required for SDH inhibition and for neoplastic growth. Indeed, we observed that, following ERK activation by PDGF treatment, TRAP1 knockout cells expressing the S568A TRAP1 mutant inhibited the SQR enzymatic activity of SDH less than cells expressing wild-type TRAP1 (Figure 6D) and that tumorigenicity was inhibited or delayed in cells expressing TRAP1 mutants (Figures 6E and 6F). Finally, we detected a high level of expression of TRAP1, HIF-1α, and PKM2, a HIF-1α transcriptional target that contributes to the metabolic switch toward an aerobic glycolysis phenotype (Li et al., 2014), in plexiform neurofibroma samples that are characterized by strong ERK1/2 activation (Figure 6G). These data highlight the oncogenic role played by a mitochondrial signaling axis involving ERK1/2, TRAP1, and SDH.

DISCUSSION

Activating mutations of the proto-oncogene Ras (Karnoub and Weinberg, 2008; Pylayeva-Gupta et al., 2011) and of its downstream effector Raf (Lavoie and Therrien, 2015) as well as homozygous loss-of-function mutations of the Ras-GAP neurofibromin (Ratner and Miller, 2015) are observed in a high proportion of tumor types, where deregulated activation of Ras/ERK signaling crucially contributes to neoplastic growth. Intensive efforts have been devoted to dissecting the changes elicited in a variety of molecular circuitries by hyperactivation of this transduction pathway. Nonetheless, an in-depth dissection of the mechanisms by which the Ras/ERK pathway takes part in the metabolic changes of tumor cells (White, 2013) is still missing, and the importance of such changes for tumor growth is unclear. Moreover, very little is known about the role played by the mitochondrial branch of Ras/ERK signaling in the process of neoplastic progression. Key findings of the present work are the identification of a fraction of active ERK1/2 inside the mitochondria of cells lacking neurofibromin and the demonstration that this mitochondrial ERK1/2 prompts a pro-neoplastic metabolic switch upon its interaction with the mitochondrial chaperone TRAP1.

We had previously shown (Rasola et al., 2010) that, in several tumor cell types, the mitochondrial fraction of ERK1/2 inhibits the permeability transition pore, a channel whose opening commits

(B) TRAP1 immunoprecipitation from $Nf1^{-/-}$ MEF mitochondria; where indicated, mitochondria were treated with the wide-spectrum kinase inhibitor staurosporine (STS, 5 μM, 15 min).

(C) Blue native gel electrophoresis performed on mitochondria isolated from $Nf1^{+/+}$ and $Nf1^{-/-}$ MEFs. Bands corresponding to complex II (CII or SDH) were cut, run on an SDS-PAGE, and probed with anti- SDHB, anti-phospho-ERK1/2, and anti-TRAP1 antibodies.

(D–G) Analysis of the SQR enzymatic activity of SDH in $Nf1^{+/+}$ and $Nf1^{-/-}$ MEFs (D), in $Nf1^{-/-}$ MEFs that underwent serum starvation for 2 hr and were then treated with PDGF (10 ng/ml) (E) or that expressed the dominant-negative mutant K52R ERK2 (F), and in $Nf1^{+/+}$ MEFs expressing MEK1-CA (G).

(H) Crosslinking experiments on mitochondria from U87 glioblastoma cells. TRAP1 was immunoprecipitated after mitochondrial treatment with the crosslinker DTBP; samples were then loaded in parallel on separate lanes of a SDS-PAGE. In the top part of the Figure, red arrowheads highlight crosslinked proteins; in the bottom part, crosslinked immunoprecipitates were cleaved by reducing DTBP with DTT, and separated proteins are indicated by blue arrowheads.

(I) Analysis of the SQR enzymatic activity of SDH in U87 glioblastoma cells either transduced with a scramble vector (SCR) or expressing the dominant-negative mutant K52R ERK2.

Data are reported as mean ± SD values ($n \geq 3$); asterisks indicate significant differences (***$p < 0.01$, *$p < 0.05$; Student's t test analysis). See also Figure S3.

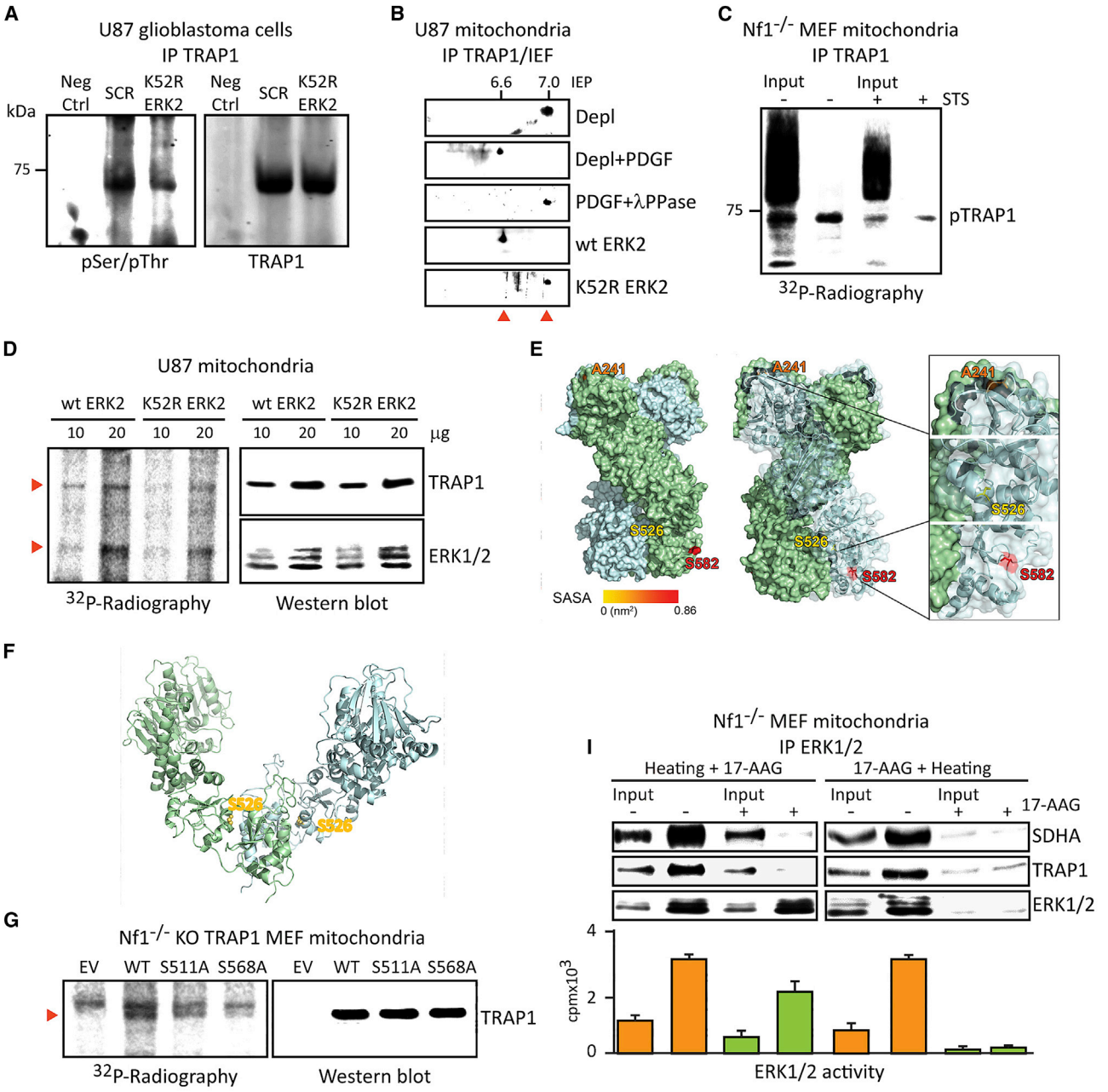

(legend on next page)

cells to death (Rasola and Bernardi, 2007), by regulating a signaling axis that involves GSK3 and the chaperone cyclophilin D. Hence, mitochondrial ERK could crucially contribute to the ability of escaping cell death that characterizes malignant cells. Our present data indicate that mitochondrial ERK plays another oncogenic role by regulating the bioenergetic changes occurring during neoplastic growth. A crucial pro-neoplastic metabolic adaptation is pseudohypoxia; i.e., oxygen-independent activation of the transcription programs mastered by HIF-1 that promote epithelial-to-mesenchymal transition, angiogenesis, and metabolic, Warburg-like adaptations (LaGory and Giaccia, 2016; Semenza, 2013), thus equipping cells to face shortages of oxygen or nutrients. Subsets of pseudohypoxic cells might be selected to advance through the early phases of neoplastic progression or to switch to a malignant phenotype under the pressure of local environmental factors, such as increasing distance from the microvessel network. It is conceivable that these adaptive changes must be flexibly regulated and that this may occur, at least in part, at a post-transcriptional level. This type of adaptation could be particularly important in shaping the oncogenic properties of tumors like neurofibromas, whose progression and clinical course result from complex heterotypic interactions among different cell types (Lin and Gutmann, 2013; Ratner and Miller, 2015) that go beyond the genotype/phenotype correlation with mutations causing loss of neurofibromin.

The mitochondrial chaperone TRAP1 plays a pivotal role in establishing the pseudohypoxic condition discussed above. TRAP1 inhibits SDH activity, and the resulting increase in intracellular succinate levels inhibits the prolyl hydroxylases responsible for dispatching HIF-1α to the proteasome for degradation (Sciacovelli et al., 2013). Here we connect this oncogenic function of TRAP1 to activation of Ras/ERK signaling. We have demonstrated that active ERK1/2 directly interacts with TRAP1 and SDH in mitochondria of cells, where this signaling axis is aberrantly activated by the absence of neurofibromin. TRAP1 is likely to play an important chaperone function in the maintenance of this molecular platform because it is able to maintain the binding with both ERK1/2 and SDHA even under stress conditions such as heat shock and to keep ERK1/2 enzymatically active. Furthermore, the association between TRAP1 and ERK1/2 is disrupted following blockade of the TRAP1 chaperone cycle. It is intriguing that, on one hand, TRAP1 acts as a chaperone on ERK1/2 and, on the other hand, ERK1/2 phosphorylates TRAP1. By a molecular dynamics simulation we have identified two putative TRAP1 residues that are targeted by ERK, Ser511 and Ser568, which have then been confirmed as bona fide ERK phosphorylation targets by in vitro kinase assays. Formation of this mitochondrial multimeric complex is increased following ERK1/2 activation, as shown by co-immunoprecipitation, blue native (BN)-PAGE, and gel filtration experiments, and directly influences the bioenergetic features of tumor cells. Indeed, we found that the SQR enzymatic activity of SDH is decreased in an ERK1/2-dependent way and that ERK-dependent phosphorylation of TRAP1 is required for SDH inhibition. Moreover, our findings that both ERK1/2 inhibition and TRAP1 ablation increase the oxygen consumption rate and coupled respiration and respiratory reserve, moving cell metabolism away from a Warburg-like phenotype, further highlight the bioenergetic importance of this regulatory mechanism.

The interaction among ERK1/2, TRAP1, and SDH has crucial consequences for cell tumorigenicity. Immortalized MEFs constitute an ideal model to analyze oncogenic effects downstream of hyperactivation of Ras/ERK signaling because its induction is sufficient to confer cell transformation ability (Hahn et al., 1999). Accordingly, we observe that ERK1/2 activation, either following neurofibromin loss or expression of a constitutively active MEK1, is mandatory for MEF transformation, which is totally lost following ERK1/2 inhibition. Notably, in this cell model, TRAP1 ablation completely abrogates neoplastic growth. In accord with our previous model of a TRAP1-driven

Figure 4. TRAP1 is Phosphorylated in an ERK-Dependent Way

(A) Western immunoblot showing Ser/Thr phosphorylation of a band co-localizing with immunoprecipitated TRAP1 from U87 glioblastoma cells. Ser/Thr phosphorylation is inhibited in cells expressing the dominant-negative mutant K52R ERK2.

(B) Isoelectrofocusing analysis performed after TRAP1 immunoprecipitation from mitochondria of U87 glioblastoma cells. The isoelectric point (IEP) of TRAP1 was around 7.0 when ERK1/2 was inhibited by serum depletion or by expression of the dominant-negative mutant K52R ERK2 or when samples were treated with PPase. The TRAP1 IEP shifted to 6.6 when ERK1/2 was activated by cell treatment with PDGF, as shown in Figure 2A, or after expression of wild-type ERK2. Orange arrowheads highlight TRAP1 spots.

(C) Autoradiography following an in vitro kinase assay performed on the TRAP1 immunoprecipitation shown in Figure 3B.

(D) Autoradiography and western immunoblot analyses of mitochondria from U87 glioblastoma cells expressing either FLAG-wild-type ERK2 or the dominant-negative mutant FLAG-K52R ERK2. As reported, in each lane pair were loaded either 10 or 20 μg of mitochondrial lysate. Orange arrowheads indicate TRAP1 and ERK1/2.

(E) Location of the predicted phospho sites on the 3D structure of TRAP1 from *Danio rerio*. The accessible surface of each of the three sites is colored from yellow to red according to the average solvent accessibility calculated in the molecular dynamics simulations. The two monomers are shown in green and cyan, respectively.

(F) Predicted location of S526 in the apo structure of TRAP1 from *Danio rerio*.

(G) Autoradiography performed on mitochondria from Nf1$^{-/-}$ MEFs transduced with an empty vector (EV) or with constructs expressing wild-type or S511A or S568A human TRAP1 cDNA after endogenous TRAP1 had been knocked out by a CRISPR/Cas9 approach. Phosphorylation of a band corresponding to TRAP1 is highlighted by the orange arrowhead.

(H) Gel filtration chromatography analysis of TRAP1, ERK1/2, and SDHA distribution in mitochondria of *Nf1*$^{-/-}$ MEFs expressing the S511A TRAP1 mutant. Mitochondrial extracts were either left untreated (top) or underwent an IVKA (bottom).

(I) Western immunoblot analysis of input and ERK1/2 immunoprecipitates from mitochondria of Nf1$^{-/-}$ MEFs. Left: mitochondrial samples were heated at 55°C for 3 min and then exposed to 17-AAG for 15 min. Right: 17-AAG was added before heating. Bar graphs indicate ERK1/2 activity measured in an in vitro kinase assay carried out on the corresponding samples reported in the blot.

See also Figure S4.

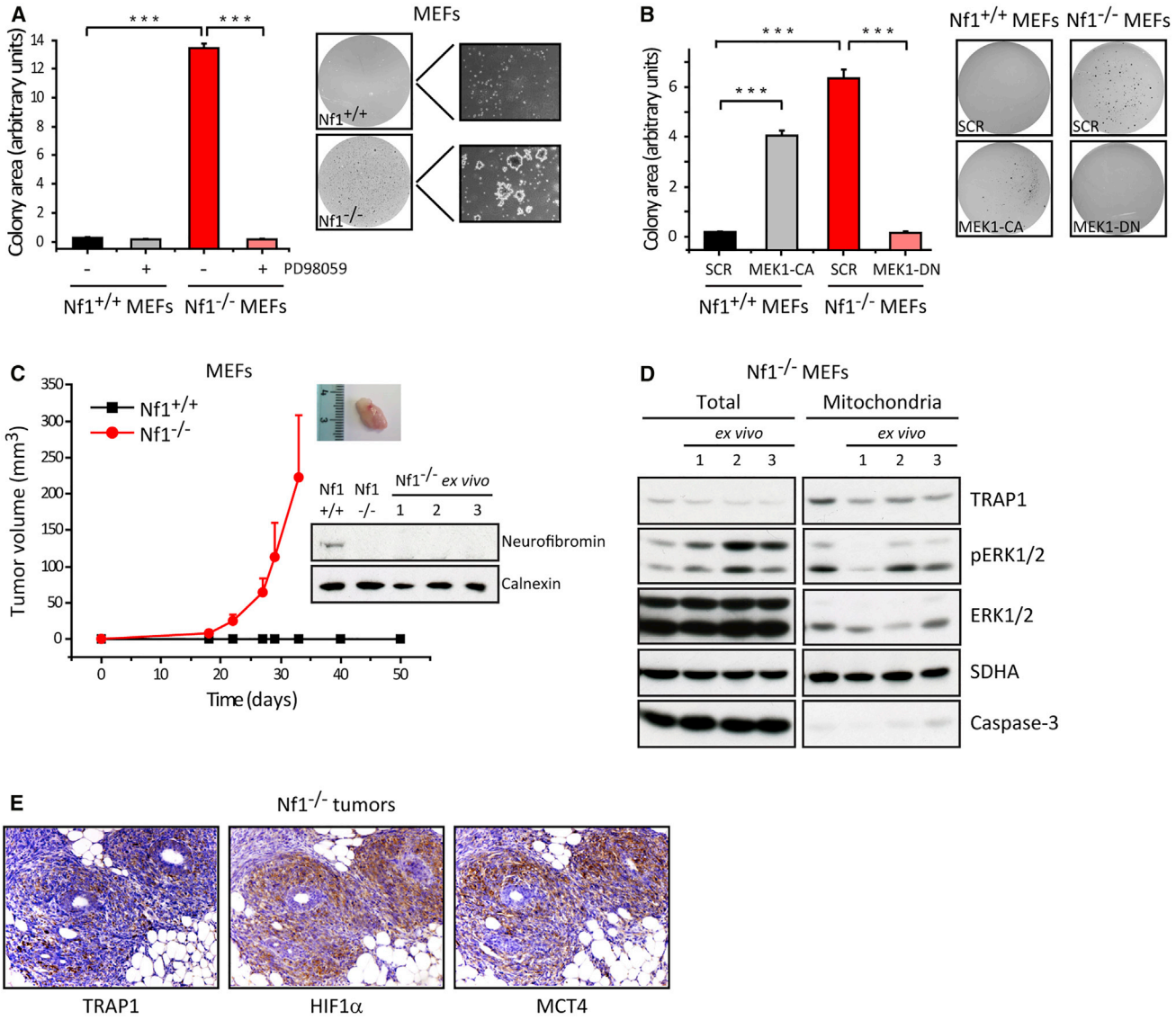

Figure 5. Activation of ERK1/2 Signaling Is Mandatory for the Tumorigenicity of Cells Lacking Neurofibromin

(A and B) Modulation of soft agar growth in $Nf1^{+/+}$ and $Nf1^{-/-}$ MEFs by the MEK inhibitor PD98059 (A) and by expression of MEK1-CA and MEK1-DN proteins (B).

(C) Kinetics of tumor growth in SCID mice after injection of $Nf1^{+/+}$ and $Nf1^{-/-}$ MEFs; a representative tumor from $Nf1^{-/-}$ MEFs is shown as an inset. Cells extracted from tumor samples lack neurofibromin expression.

(D) Western immunoblot of tumor samples obtained following injection of $Nf1^{-/-}$ MEFs in nude mice showing the mitochondrial expression of TRAP1, active ERK1/2, and SDH. Caspase-3 was used as a cytosolic marker.

(E) Immunohistochemical inspections of serial sections of $Nf1^{-/-}$ MEF tumors reveal the presence and co-localization of TRAP1, HIF-1α, and the HIF-1α metabolic target MCT4.

In (A)–(C), data are reported as mean ± SD values ($n \geq 3$); asterisks indicate significant differences (***$p < 0.01$, Student's t test analysis). See also Figures S5 and S6.

pseudohypoxic signaling axis, TRAP1-bearing xenograft tumors display HIF-1α stabilization, and succinate can reinstate the tumorigenicity of cells lacking TRAP1, but not when prolyl hydroxylases are activated by α-ketoglutarate. In addition, here we also observe that cells expressing TRAP1 mutants that cannot be phosphorylated in an ERK-dependent way become unable to undergo neoplastic growth. This result highlights the oncogenic importance of the mitochondrial interaction between ERK1/2 and TRAP1 and indicates that TRAP1 is a pro-neoplastic metabolic effector of Ras/ERK signaling.

It must be underlined here that we also find TRAP1 and active ERK1/2 in mitochondria of other neoplastic cells endowed with loss of neurofibromin, such as neurofibroma samples, where we also observe induction of HIF1α and of its downstream metabolic effectors, or U87 human glioblastoma cells, where TRAP1 ablation has the same anti-neoplastic effect observed in MEFs.

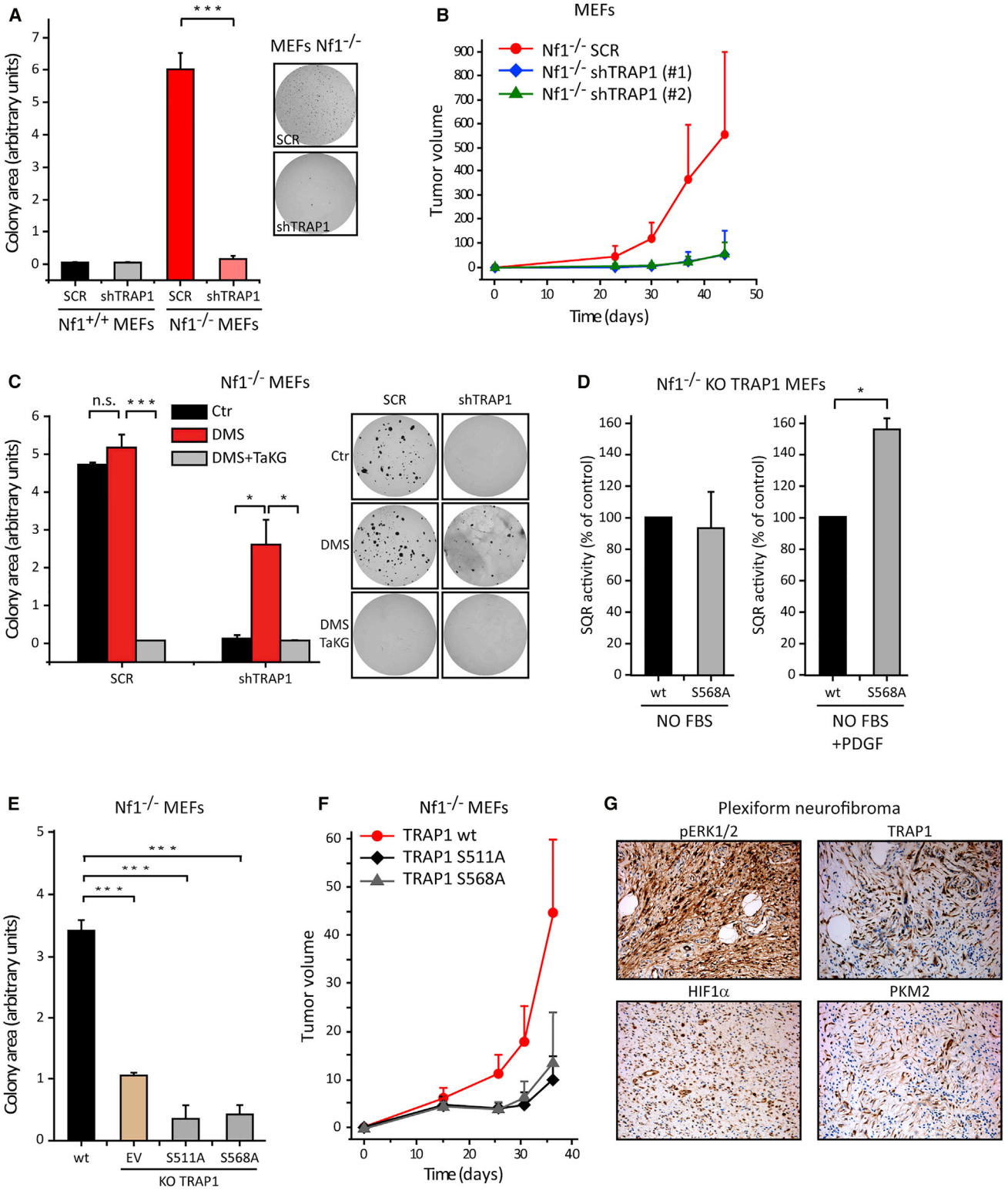

Figure 6. TRAP1 Is Required for the Tumorigenicity of Cells Lacking Neurofibromin through ERK-Dependent Inhibition of SDH

(A) Inhibition of soft agar growth in Nf1$^{-/-}$ MEFs following ablation of TRAP1 expression through RNAi (shTRAP1 cells).

(B) Kinetics of tumor growth in SCID mice after injection of Nf1$^{-/-}$ MEFs with or without TRAP1.

(legend continued on next page)

Hence, this study suggests that TRAP1 regulation by mitochondrial ERK1/2 is a major regulatory pathway for the oncogenic role of the chaperone and that it could be a general mechanism of rapid and flexible metabolic tuning shared by cells characterized by oncogenic activation of Ras/ERK signaling. This possibility is strengthened by recent observations indicating that TRAP1 is regulated in several ways at the post-translational level (Condelli et al., 2015; Kowalik et al., 2016; Rizza et al., 2016). These subtle and complex mechanisms of modulation of TRAP1 activity, together with its changes in expression depending on the tumor type and stage, might also explain the reported contrasting effects of the chaperone on the neoplastic process (Yoshida et al., 2013; for a thorough discussion see Rasola et al., 2014). Moreover, our data do not exclude the possibility that TRAP1 also contributes to the tumorigenicity of cells by mechanisms other than pseudohypoxic stabilization of HIF1α and, perhaps, different from bioenergetic changes because it is plausible that TRAP1 interacts with multiple mitochondrial clients.

Our results identify a mechanistic connection between deregulated Ras/ERK signaling and the pro-neoplastic metabolic switch orchestrated by TRAP1, demonstrating that active ERK1/2 interacts with TRAP1 and SDH in the mitochondria of neurofibromin-deficient cells and that ERK-dependent phosphorylation of specific residues on TRAP1 has a key oncogenic role. It is important to note that, in several tumor types, TRAP1 expression is strongly induced (Kang et al., 2007), sometimes from the very early stages of neoplastic growth (Kowalik et al., 2016), making it a suitable and promising target for the development of novel anti-tumor strategies that could have few negative effects on non-transformed tissues.

EXPERIMENTAL PROCEDURES

Detailed methods can be found in the Supplemental Experimental Procedures.

Cells and Tissue Samples

Experiments were performed on wild-type and Nf1 knockout MEFs and human U87 glioblastoma cells. TRAP1 expression was knocked down by stable transfection with short hairpin RNAs (shRNAs) or knocked out with a CRISPR/Cas9 approach. pBABE vectors were used for expression of CA (S217E/S221E) and DN (S217A) MEK1; pFLAG vectors were used for expression of the wild-type or kinase-dead (K52R) ERK2 mutant. The QuikChange site-directed mutagenesis kit (Stratagene) was used to generate TRAP1 mutants. Tissue samples from human plexiform neurofibromas were obtained from patients diagnosed with NF1 during surgical cancer removal after express written informed consent. Immunohistochemical analysis was performed in accordance with the declaration of Helsinki and following the regulation of the Padova Hospital Ethical Committee.

Tumorigenesis Assays

Cell tumorigenicity was assessed both in vitro, with assays of growth in soft agar or in Matrigel, and in vivo following cell injection in severe combined immunodeficiency (SCID) mice.

Cytofluorimetric Analyses

Cytofluorimetric analyses were utilized to measure cell death with the use of Annexin V-fluorescein isothiocyanate (FITC) and propidium iodide probes as well as mitochondrial mass with the use of nonyl acridine orange and mitochondrial membrane potential with the tetramethylrhodamine methyl ester (TMRM) dye.

Mitochondrion Purification

Mitochondria were isolated through sequential centrifugations after mechanical cell disruption. To eliminate cytosolic contaminants, isolated mitochondria were partially digested with different concentrations of trypsin.

Biochemical Analyses

Western immunoblot and immunoprecipitation experiments were performed following standard techniques. BN-PAGE experiments were carried out on mitochondria to isolate electron transport chain (ETC) complexes. After a first electrophoresis under non-denaturing conditions, bands were visualized with Coomassie blue staining, cut, and run on SDS-PAGE for protein identification by western immunoblot. Crosslinking assays were performed on isolated mitochondria incubated with the membrane-permeable, homobifunctional reagent dimethyl 3,3′-dithiobis-propionimidate (DTBP) prior to immunoprecipitation. Isoelectrofocusing experiments were conducted on mitochondria after TRAP1 immunoprecipitation. First-dimension electrophoreses were carried out using linear pH gradient strips and were followed by SDS-PAGE and western immunoblot. Gel filtration chromatographies were carried out following standard techniques by using fast protein liquid chromatography (FPLC) Superdex S200 columns. In vitro kinase assays were carried out by labeling mitochondria with [γ-^{32}P]-ATP. Phosphate incorporation was assessed by autoradiography.

Measurement of SQR Activity of SDH

The SQR activity of SDH was measured with classical spectrophotometric approaches on cell or mitochondrial lysates. Each measurement of respiratory chain (RC) complex activity was normalized for protein amount and for citrate synthase activity.

Measurements of OCR and ECAR

In vivo respiration and the glycolytic pathway were followed in a kinetic mode by measuring the OCR and extracellular acidification rate (ECAR) of cell monolayers with an extracellular flux analyzer (Seahorse Biosciences).

Immunohistochemical Analyses

Immunohistochemical inspections were performed on serial sections of paraffin-embedded tumor samples following standard procedures.

Intracellular ATP Determination

Intracellular ATP was quantified by the luciferin/luciferase method. Cells were kept for 2 hr under the different experimental conditions.

(C) Modulation of soft agar growth in Nf1$^{-/-}$ MEFs with or without TRAP1 by the cell-permeable succinate analog DMS (0.5 mM) and by the cell-permeable esterified form of a-ketoglutarate (TaKG, 1 mM).
(D) Analysis of the SQR enzymatic activity of SDH in Nf1$^{-/-}$ MEFs where the endogenous TRAP1 had been knocked out through a CRISPR/Cas9 approach and either wild-type or mutant (S568A) human TRAP1 were re-expressed (Figure 4G). SQR activity was assessed in cells that underwent serum starvation for 2 hr (left) and that were then treated with PDGF (10 ng/ml, right).
(E) Inhibition of colony growth in Matrigel in Nf1$^{-/-}$ MEFs where TRAP1 had been knocked out as in (D) and human TRAP1 mutants (S511A or S568A) were re-expressed. Expression of wild-type human TRAP1 restored colony growth.
(F) Kinetics of in vivo tumor growth of Nf1$^{-/-}$ MEFs expressing either the wild-type TRAP1 or TRAP1 mutants S511A or S568A.
(G) Immunohistochemical inspections of serial sections of a representative human plexiform neurofibroma reveal the presence and co-localization of phospho-ERK1/2, TRAP1, HIF-1α, and the HIF-1α metabolic target PKM2.
Data are reported as mean ± SD values ($n \geq 3$); asterisks indicate significant differences (***$p < 0.01$, *$p < 0.05$; Student's t test analysis). Tumor volume is expressed in cubic millimeters. See also Figure S6.

Molecular Dynamics Simulations

Molecular dynamics simulations were performed using GROMACS 4.6 (http://www.gromacs.org). The X-ray structure of TRAP1 was solved in the presence of the ATP analog adenylyl-imidodiphosphate (AMP-PNP), which was removed for modeling the apo variant. The models of the ADP and ATP-bound states of TRAP1 were generated using Modeler, whereas $\Delta\Delta G$ calculations were carried out with the FoldX suite (http://foldxsuite.crg.eu/).

Statistical Analysis

Student's t test was used to compare pairs of data groups. ANOVA followed by Bonferroni post hoc test was used for multiple comparisons. In all figures, bar graphs report mean ± SD values ($n \geq 3$); *$p < 0.05$, ***$p < 0.01$.

SUPPLEMENTAL INFORMATION

Supplemental Information includes Supplemental Experimental Procedures, six figures, and one table and can be found with this article online at http://dx.doi.org/10.1016/j.celrep.2016.12.056.

AUTHOR CONTRIBUTIONS

Conceptualization, I.M. and A.R.; Visualization, I.M., M.L., and A.R.; Methodology, I.M., F. Ciscato, A.M.B., F. Chiara, and E.P.; Investigation, I.M., F. Ciscato, E.T., M.C., F. Chiara, G.C., M.L., G.G., A.G., M.P., V.G., and S.E.V.; Formal Analysis, E.P. and M.L.; Resources, A.M.B., S.I., F. Chiara, E.P., M.R., F. Calabrese, P.B., and A.R.; Writing – Original Draft, A.R.; Writing – Review and Editing, I.M., S.I., F. Chiara, E.P., P.B., and A.R.; Funding Acquisition, P.B. and A.R.; Project Administration, A.R.

ACKNOWLEDGMENTS

We thank Reuven Stein for MEFs; Luca Scorrano for the pBABE-MEK1-CA and pBABE-MEK1-DN vectors; Zhimin Lu for the pFLAG wild-type and kinase-dead (K52R) ERK2 vectors; Diego De Stefani for the pMDLg/pRRE, pRSV-Rev and pMD2.G plasmids; Elena Trevisan for technical assistance; and our system operator Marco Ardina for inexhaustible help. This work was supported by Associazione Italiana Ricerca sul Cancro Grants IG15863 (to A.R.) and IG17067 (to P.B.) and University of Padova Grant Progetto di Ateneo CPDA123598/12 (to A.R). I.M. was supported by a research grant from the University of Padova and by Associazione LINFA Onlus.

Received: June 30, 2016
Revised: November 4, 2016
Accepted: December 18, 2016
Published: January 17, 2017

REFERENCES

Ahearn, I.M., Haigis, K., Bar-Sagi, D., and Philips, M.R. (2011). Regulating the regulator: post-translational modification of RAS. Nat. Rev. Mol. Cell Biol. *13*, 39–51.

Barbosa, I.A., Machado, N.G., Skildum, A.J., Scott, P.M., and Oliveira, P.J. (2012). Mitochondrial remodeling in cancer metabolism and survival: potential for new therapies. Biochim. Biophys. Acta *1826*, 238–254.

Bardella, C., Pollard, P.J., and Tomlinson, I. (2011). SDH mutations in cancer. Biochim. Biophys. Acta *1807*, 1432–1443.

Barkan, B., Starinsky, S., Friedman, E., Stein, R., and Kloog, Y. (2006). The Ras inhibitor farnesylthiosalicylic acid as a potential therapy for neurofibromatosis type 1. Clin. Cancer Res. *12*, 5533–5542.

Blum, R., Jacob-Hirsch, J., Amariglio, N., Rechavi, G., and Kloog, Y. (2005). Ras inhibition in glioblastoma down-regulates hypoxia-inducible factor-1alpha, causing glycolysis shutdown and cell death. Cancer Res. *65*, 999–1006.

Boroughs, L.K., and DeBerardinis, R.J. (2015). Metabolic pathways promoting cancer cell survival and growth. Nat. Cell Biol. *17*, 351–359.

Brems, H., Beert, E., de Ravel, T., and Legius, E. (2009). Mechanisms in the pathogenesis of malignant tumours in neurofibromatosis type 1. Lancet Oncol. *10*, 508–515.

Cancer Genome Atlas Research Network (2008). Comprehensive genomic characterization defines human glioblastoma genes and core pathways. Nature *455*, 1061–1068.

Cecchini, G. (2003). Function and structure of complex II of the respiratory chain. Annu. Rev. Biochem. *72*, 77–109.

Condelli, V., Maddalena, F., Sisinni, L., Lettini, G., Matassa, D.S., Piscazzi, A., Palladino, G., Amoroso, M.R., Esposito, F., and Landriscina, M. (2015). Targeting TRAP1 as a downstream effector of BRAF cytoprotective pathway: a novel strategy for human BRAF-driven colorectal carcinoma. Oncotarget *6*, 22298–22309.

Dhillon, A.S., Hagan, S., Rath, O., and Kolch, W. (2007). MAP kinase signalling pathways in cancer. Oncogene *26*, 3279–3290.

Hahn, W.C., Counter, C.M., Lundberg, A.S., Beijersbergen, R.L., Brooks, M.W., and Weinberg, R.A. (1999). Creation of human tumour cells with defined genetic elements. Nature *400*, 464–468.

Hoekstra, A.S., and Bayley, J.P. (2013). The role of complex II in disease. Biochim. Biophys. Acta *1827*, 543–551.

Hollstein, P.E., and Cichowski, K. (2013). Identifying the Ubiquitin Ligase complex that regulates the NF1 tumor suppressor and Ras. Cancer Discov. *3*, 880–893.

Jessen, W.J., Miller, S.J., Jousma, E., Wu, J., Rizvi, T.A., Brundage, M.E., Eaves, D., Widemann, B., Kim, M.O., Dombi, E., et al. (2013). MEK inhibition exhibits efficacy in human and mouse neurofibromatosis tumors. J. Clin. Invest. *123*, 340–347.

Kang, B.H., Plescia, J., Dohi, T., Rosa, J., Doxsey, S.J., and Altieri, D.C. (2007). Regulation of tumor cell mitochondrial homeostasis by an organelle-specific Hsp90 chaperone network. Cell *131*, 257–270.

Karnoub, A.E., and Weinberg, R.A. (2008). Ras oncogenes: split personalities. Nat. Rev. Mol. Cell Biol. *9*, 517–531.

Kowalik, M.A., Guzzo, G., Morandi, A., Perra, A., Menegon, S., Masgras, I., Trevisan, E., Angioni, M.M., Fornari, F., Quagliata, L., et al. (2016). Metabolic reprogramming identifies the most aggressive lesions at early phases of hepatic carcinogenesis. Oncotarget *7*, 32375–32393.

Krukenberg, K.A., Street, T.O., Lavery, L.A., and Agard, D.A. (2011). Conformational dynamics of the molecular chaperone Hsp90. Q. Rev. Biophys. *44*, 229–255.

LaGory, E.L., and Giaccia, A.J. (2016). The ever-expanding role of HIF in tumour and stromal biology. Nat. Cell Biol. *18*, 356–365.

Lavery, L.A., Partridge, J.R., Ramelot, T.A., Elnatan, D., Kennedy, M.A., and Agard, D.A. (2014). Structural asymmetry in the closed state of mitochondrial Hsp90 (TRAP1) supports a two-step ATP hydrolysis mechanism. Mol. Cell *53*, 330–343.

Lavoie, H., and Therrien, M. (2015). Regulation of RAF protein kinases in ERK signalling. Nat. Rev. Mol. Cell Biol. *16*, 281–298.

Leskovar, A., Wegele, H., Werbeck, N.D., Buchner, J., and Reinstein, J. (2008). The ATPase cycle of the mitochondrial Hsp90 analog Trap1. J. Biol. Chem. *283*, 11677–11688.

Li, Z., Yang, P., and Li, Z. (2014). The multifaceted regulation and functions of PKM2 in tumor progression. Biochim. Biophys. Acta *1846*, 285–296.

Lin, A.L., and Gutmann, D.H. (2013). Advances in the treatment of neurofibromatosis-associated tumours. Nat. Rev. Clin. Oncol. *10*, 616–624.

Malone, C.F., Fromm, J.A., Maertens, O., DeRaedt, T., Ingraham, R., and Cichowski, K. (2014). Defining key signaling nodes and therapeutic biomarkers in NF1-mutant cancers. Cancer Discov. *4*, 1062–1073.

Masgras, I., Rasola, A., and Bernardi, P. (2012). Induction of the permeability transition pore in cells depleted of mitochondrial DNA. Biochim. Biophys. Acta *1817*, 1860–1866.

Poderoso, C., Converso, D.P., Maloberti, P., Duarte, A., Neuman, I., Galli, S., Cornejo Maciel, F., Paz, C., Carreras, M.C., Poderoso, J.J., and Podestá,

E.J. (2008). A mitochondrial kinase complex is essential to mediate an ERK1/2-dependent phosphorylation of a key regulatory protein in steroid biosynthesis. PLoS ONE *3*, e1443.

Pridgeon, J.W., Olzmann, J.A., Chin, L.S., and Li, L. (2007). PINK1 protects against oxidative stress by phosphorylating mitochondrial chaperone TRAP1. PLoS Biol. *5*, e172.

Pylayeva-Gupta, Y., Grabocka, E., and Bar-Sagi, D. (2011). RAS oncogenes: weaving a tumorigenic web. Nat. Rev. Cancer *11*, 761–774.

Rasola, A., and Bernardi, P. (2007). The mitochondrial permeability transition pore and its involvement in cell death and in disease pathogenesis. Apoptosis *12*, 815–833.

Rasola, A., Sciacovelli, M., Chiara, F., Pantic, B., Brusilow, W.S., and Bernardi, P. (2010). Activation of mitochondrial ERK protects cancer cells from death through inhibition of the permeability transition. Proc. Natl. Acad. Sci. USA *107*, 726–731.

Rasola, A., Neckers, L., and Picard, D. (2014). Mitochondrial oxidative phosphorylation TRAP(1)ped in tumor cells. Trends Cell Biol. *24*, 455–463.

Ratner, N., and Miller, S.J. (2015). A RASopathy gene commonly mutated in cancer: the neurofibromatosis type 1 tumour suppressor. Nat. Rev. Cancer *15*, 290–301.

Rizza, S., Montagna, C., Cardaci, S., Maiani, E., Di Giacomo, G., Sanchez-Quiles, V., Blagoev, B., Rasola, A., De Zio, D., Stamler, J.S., et al. (2016). S-nitrosylation of the mitochondrial chaperone TRAP1 sensitizes hepatocellular carcinoma cells to inhibitors of succinate dehydrogenase. Cancer Res. *76*, 4170–4182.

Sciacovelli, M., Guzzo, G., Morello, V., Frezza, C., Zheng, L., Nannini, N., Calabrese, F., Laudiero, G., Esposito, F., Landriscina, M., et al. (2013). The mitochondrial chaperone TRAP1 promotes neoplastic growth by inhibiting succinate dehydrogenase. Cell Metab. *17*, 988–999.

See, W.L., Tan, I.L., Mukherjee, J., Nicolaides, T., and Pieper, R.O. (2012). Sensitivity of glioblastomas to clinically available MEK inhibitors is defined by neurofibromin 1 deficiency. Cancer Res. *72*, 3350–3359.

Selak, M.A., Armour, S.M., MacKenzie, E.D., Boulahbel, H., Watson, D.G., Mansfield, K.D., Pan, Y., Simon, M.C., Thompson, C.B., and Gottlieb, E. (2005). Succinate links TCA cycle dysfunction to oncogenesis by inhibiting HIF-alpha prolyl hydroxylase. Cancer Cell *7*, 77–85.

Semenza, G.L. (2013). HIF-1 mediates metabolic responses to intratumoral hypoxia and oncogenic mutations. J. Clin. Invest. *123*, 3664–3671.

Shapira, S., Barkan, B., Friedman, E., Kloog, Y., and Stein, R. (2007). The tumor suppressor neurofibromin confers sensitivity to apoptosis by Ras-dependent and Ras-independent pathways. Cell Death Differ. *14*, 895–906.

Shiau, A.K., Harris, S.F., Southworth, D.R., and Agard, D.A. (2006). Structural Analysis of E. coli hsp90 reveals dramatic nucleotide-dependent conformational rearrangements. Cell *127*, 329–340.

White, E. (2013). Exploiting the bad eating habits of Ras-driven cancers. Genes Dev. *27*, 2065–2071.

Yang, M., Soga, T., and Pollard, P.J. (2013). Oncometabolites: linking altered metabolism with cancer. J. Clin. Invest. *123*, 3652–3658.

Yap, Y.S., McPherson, J.R., Ong, C.K., Rozen, S.G., Teh, B.T., Lee, A.S., and Callen, D.F. (2014). The NF1 gene revisited - from bench to bedside. Oncotarget *5*, 5873–5892.

Yoshida, S., Tsutsumi, S., Muhlebach, G., Sourbier, C., Lee, M.J., Lee, S., Vartholomaiou, E., Tatokoro, M., Beebe, K., Miyajima, N., et al. (2013). Molecular chaperone TRAP1 regulates a metabolic switch between mitochondrial respiration and aerobic glycolysis. Proc. Natl. Acad. Sci. USA *110*, E1604–E1612.

Zhu, J.H., Guo, F., Shelburne, J., Watkins, S., and Chu, C.T. (2003). Localization of phosphorylated ERK/MAP kinases to mitochondria and autophagosomes in Lewy body diseases. Brain Pathol. *13*, 473–481.